



Identification of the Induction Machine Electromagnetic Substitute Parameters for Transient Process Analysis in a Standstill and Practical Determination of Rotor Winding Temperature Rise

Zdeněk Čerovský^{id}, Pavel Koblre^{id}, Miroslav Lev^{id}

Department of Electric Drives and Traction, Czech Technical University in Prague, Faculty of Electrical Engineering

Cite this article as: Z. Čerovský, P. Koblre, and M. Lev, "Identification of the induction machine electromagnetic substitute parameters for transient process analysis in a standstill and practical determination of rotor winding temperature rise," *Electrica*, 24(3), 682-692, 2024.

ABSTRACT

This paper deals with the parameter identification of induction machine rotor and stator windings. These two magnetically coupled circuits are described and analyzed to explain the novel method that can identify the set of substitute parameters (not equivalent circuit parameters) which can be used for some analysis of transient processes in a stationary induction machine. The parameters are: inductive leakage factor, substitute rotor resistance, substitute rotor inductance, and substitute mutual inductance. The method belongs to the group of so-called off-line methods, i.e., it is performed on a machine in a standstill, and it assumes a star-connected induction motor. The correctness of the method is verified by calculation as well as by measurement. Moreover, the practical use of the method is shown in an example of how to determine the rotor winding temperature rise, and the results of the measurement on an induction motor with a power of 0.75 kW are presented. The method can be performed even when the rotor circuit is hidden inside the completely closed rotor construction, as in the case of a squirrel cage induction motor, i.e., without access to the rotor circuit.

Index Terms—Induction machine, parameters identification, temperature rise measurement

Corresponding author:

Pavel Koblre

E-mail:

koblrpav@fel.cvut.cz

Received: December 14, 2023

Revision Requested: February 16, 2024

Last Revision Received: July 29, 2024

Accepted: September 4, 2024

Publication Date: October 15, 2024

DOI: 10.5152/electrica.2024.23196



Content of this journal is licensed under a Creative Commons Attribution-NonCommercial 4.0 International License.

I. INTRODUCTION

Many papers deal with the identification of rotor winding parameters in induction machines [1-4]. Transient phenomena in electric machines were studied very carefully [5-10] and nowadays this topic still remains the focus of many researchers [11-15]. The main aim is to predict sudden short circuit currents, predict losses in machines, or predict additional straining of the machine. Several methods are usually used to calculate the machine's transient behavior. Models with lumped circuits are very common [16]. The analytical solution often omits winding resistances and uses the principle of constant magnetic flux according to Lenz's law [8]. The subtransient reactance is calculated when the magnetic flux in windings remains constant. However, the magnetic field distribution in the calculated machine is complicated. Direct calculation with the finite element method is possible but it is difficult and time-consuming [17]. Calculation programs to save time were developed [17-20]. The method to calculate the stationary inductances and equivalent circuit voltages newly implemented in FEMAG yields very good results [21]. (FEMAG is an interactive program that has been developed at ETH Zurich since 1982.)

Gained parameters of the induction machine may be used in different cases, ranging from testing of an induction machine, across diagnostics to control of an electric drive [22-24]. However, it is possible to estimate a set of substitute parameters, i.e., not real parameters, which have the property that a transient process in a braked motor with the substitute parameters gives the same response to some excitation as the braked motor with real parameters. In practice, it is required to measure the warm winding resistance and then to commonly calculate its temperature rise [25], especially in electric vehicles supplied by batteries under low voltage and higher current [26]. However, access to the winding is necessary. It is difficult, or mostly impossible, in the case when the temperature of a squirrel cage rotor of an induction motor should be measured. Therefore, a practical method to gain the rotor-winding temperature is to usually estimate the difference between the stator and rotor-winding temperature. In addition, some papers presenting different methods of rotor temperature or temperature rise estimation have already been

published. The paper [27] describes the electrical model of an induction motor combined with the thermal one, and the precise calculation of the temperature rise in a locked rotor is obtained. Thermal models are used for rotor temperature estimation quite often [28, 29]. Two superheterodyne receivers combined with MRAS are used to estimate squirrel-cage rotor temperature in [30]. The rotor temperature is calculated from the rotor resistance determined by signal injection in [31] and [32]. The paper [33] summarizes that all these methods can be divided into two groups—thermal model-based methods and parameter-based methods.

The method presented in this paper belongs to the second group, which is based on the determination of substitute parameters of the induction machine. We present an easy method for measuring of the temperature rise in the rotor winding of the induction motor in a standstill without any access to the rotor.

II. IDENTIFICATION OF SUBSTITUTE PARAMETERS

A. Problem Definition

Let us turn our attention to the induction machine stator and rotor windings. They are mutually magnetically coupled, so the rotor winding parameters influence the transient processes in the stator winding. However, the rotor winding is hidden in the rotor construction. One possible set of sought-after electromagnetic parameters of an induction machine, which is usually used, consists of the stator and rotor-winding Ohm resistance, stator and rotor-winding self-inductance, mutual inductance, and inductive leakage factor. Determining the stator parameters is generally a problem-free task. However, obtaining the other parameters accurately without access to the rotor circuit brings difficulties in general. Fortunately, some practical issues do not require knowing the rotor resistance and rotor inductance separately or independently. Thus, the question can be stated: Is it actually somehow possible to determine the rotor parameters in an exploitable form accurately without access to the rotor circuit? This chapter deals with this task.

B. Mathematical Model for Transient Processes

For the description and analysis of a transient process when a voltage step $u_s = 1 \cdot U_s$ is applied to the stator winding of the still-standing machine, the following equations can be used:

$$L_s \frac{di_s}{dt} + M \frac{di_r}{dt} + R_s \cdot i_s = u_s \quad (1)$$

$$M \frac{di_s}{dt} + L_r \frac{di_r}{dt} + R_r \cdot i_r = 0 \quad (2)$$

(1) and (2) are not the equations describing an induction motor as a whole. They are the equations describing the relation between one phase of the stator and the short-circuited squirrel cage rotor winding of a three-phase still-standing induction motor. The stator and rotor circuits have only magnetic coupling, and their parameters can be expressed only with stator self-inductance L_s , rotor self-inductance L_r , mutual inductance M , stator resistance R_s , and rotor resistance R_r .

The system of (1) and (2) can be solved with the help of the Laplace transformation [34-36]. The transformed equations are then

$$(p \cdot L_s + R_s) \cdot i_s(p) + p \cdot M \cdot i_r(p) = \frac{U_s}{p} \quad (3)$$

$$p \cdot M \cdot i_s(p) + (p \cdot L_r + R_r) \cdot i_r(p) = 0 \quad (4)$$

Let us calculate the Laplace transformation of the stator current $i_s(p)$ ([34, 35])

$$\begin{aligned} i_s(p) &= \frac{p \cdot L_r + R_r}{(L_s \cdot L_r - M^2) \cdot p^2 + (L_s \cdot R_r + L_r \cdot R_s) \cdot p + R_s \cdot R_r} \cdot \frac{U_s}{p} = \\ &= \frac{p \cdot L_r + R_r}{p \cdot \left[L_s \cdot L_r \cdot \sigma \cdot p^2 + L_s \cdot L_r \left(\frac{1}{T_s} + \frac{1}{T_r} \right) \cdot p + R_s \cdot R_r \right]} \cdot U_s \end{aligned} \quad (5)$$

The unknown parameters of an inaccessible rotor circuit in (5) are as follows:

- Inductive leakage factor σ between the stator and rotor windings [37-39]

$$\sigma = \frac{L_s \cdot L_r - M^2}{L_s \cdot L_r} \quad (6)$$

- Self-inductance L_r and resistance R_r of one phase of the rotor winding.
- The time constant of the rotor winding

$$T_r = \frac{L_r}{R_r} \quad (7)$$

As the known parameters in (5) are considered:

- Self-inductance L_s and resistance R_s of one phase of the stator winding because they can be directly measured or calculated.
- Stator time constant

$$T_s = \frac{L_s}{R_s} \quad (8)$$

A practical way to determine the stator resistance R_s is to perform the measurement with a DC voltage step on one phase of the stator winding and measure the current after a transient process is over [40].

The self-inductance of the stator phase coil L_s can be determined from a simple AC measurement during the manufacturing process when the rotor packet itself, i.e., without a cage (rotor winding), is input into the stator. A different method is to measure the three-phase stator winding impedance when the rotor rotates at synchronous speed. Because the resistance R_s is known, the three-phase stator inductance L_1 can be obtained. Knowing that the inductance L_s equals 2/3 of the three-phase stator inductance L_1 [41], L_s can be simply calculated.

The mutual inductance M can be calculated from the relation to the leakage factor σ according to (21), and the rotor time constant T_r can be obtained from (19), as shown and explained later.

C. Determination of the New Set of Parameters

To find the time function of the stator current $i_s(t)$ from $i_s(p)$ in (5), the difficult inverse Laplace transformation of that expression must be performed. A common procedure is to find the solution in a list of Laplace transform vocabulary indexes [34-36].

In our case, we use the Heaviside decomposition principle method [34], which solves the decomposition of (5) into partial fractions. After we use it, we find an identity between (5) and (9).

$$I_s(p) = \frac{A_1}{p-p_1} + \frac{A_2}{p-p_2} + \frac{A_3}{p-p_3}. \quad (9)$$

To find the time function $i_s(t)$, it is easy to use the inverse Laplace transformation of each partial fraction in (9).

We obtain the real stator current response $i_s(t)$ to the voltage step using a Laplace transform vocabulary index as

$$i_s(t) = A_1 e^{p_1 t} + A_2 e^{p_2 t} + A_3 e^{p_3 t}, \quad (10)$$

where constants p_1, p_2, p_3 are the poles of the Laplace transform $I_s(p)$ in (5).

The pole p_1 results from the denominator (5) directly, so $p_1=0$. The remaining poles, p_2 and p_3 , result from the quadratic part of the denominator and can be written in the form as follows:

$$p_{2,3} = -\frac{1}{2\sigma} \left(\frac{1}{T_s} + \frac{1}{T_r} \right) \pm \sqrt{\left[\frac{1}{2\sigma} \left(\frac{1}{T_s} + \frac{1}{T_r} \right) \right]^2 - \frac{1}{\sigma T_s T_r}}. \quad (11)$$

Each pole p_1, p_2, p_3 in (10) can be replaced with the time constant T_x , where $x=1, 2, 3$, respectively. For $p_1=0, T_1 \rightarrow \infty$. Poles p_2 and p_3 are negative, and time constants are positive, i.e., $p_x = -\frac{1}{T_x}$, so $e^{p_x t} = e^{-\frac{t}{T_x}}$.

Constants A_1, A_2, A_3 in (10) can be written according to [34] as

$$A_1 = \frac{U_s}{R_s}, \quad (12)$$

$$A_2 = \frac{U_s (L_r \cdot p_2 + R_r)}{p_2 \left[2 \cdot L_s \cdot L_r \cdot \sigma \cdot p_2 + L_s \cdot L_r \left(\frac{1}{T_s} + \frac{1}{T_r} \right) \right]}, \quad (13)$$

$$A_3 = \frac{U_s (L_r \cdot p_3 + R_r)}{p_3 \left[2 \cdot L_s \cdot L_r \cdot \sigma \cdot p_3 + L_s \cdot L_r \left(\frac{1}{T_s} + \frac{1}{T_r} \right) \right]}. \quad (14)$$

Let us substitute $p_{2,3} = a \pm b$ in (11). When $p_x = -\frac{1}{T_x}$, we can write

$$T_{2,3} = -\frac{1}{a \pm b} = \frac{-a \pm b}{a^2 - b^2}. \quad (15)$$

And because $a^2 - b^2 = \frac{1}{\sigma T_s T_r}$, we get from (11)

$$T_{2,3} = \frac{T_s + T_r}{2} \pm \sqrt{\left(\frac{T_s + T_r}{2} \right)^2 - \sigma T_s T_r}. \quad (16)$$

The relationship between constants T_2, T_3, T_s , and T_r was calculated in [16] using the assumption that $\sigma \rightarrow 0$. However, in our case, the leakage factor σ varies, so it can be higher than zero. Therefore, we shall use a more exact method to obtain the mentioned relationship.

Using (16), we have T_2 and T_3 exactly.

$$T_2 + T_3 = T_s + T_r, \quad (17)$$

$$T_2 - T_3 = 2 \sqrt{\left(\frac{T_s + T_r}{2} \right)^2 - \sigma T_s T_r}. \quad (18)$$

Because T_s is known or can be measured, we obtain T_r from (17) as

$$T_r = T_2 + T_3 - T_s. \quad (19)$$

The crucial fact is that the rotor time constant T_r is valid for the same temperature as the time constants T_2, T_3 , and T_s in (19).

From (17) and (18), we get for the leakage factor σ

$$\sigma = \frac{1}{4 T_s T_r} \left[(T_2 + T_3)^2 - (T_2 - T_3)^2 \right] = \frac{T_2 T_3}{T_s T_r}. \quad (20)$$

However, it is defined as

$$\sigma = \frac{L_s L_r - M^2}{L_s L_r} = 1 - \frac{M^2}{L_s L_r}. \quad (21)$$

We have derived the relations (17), (18), and (19) by use of the exact method for any leakage factor σ . We also have the possibility to calculate σ directly from time constants T_2, T_3, T_s , and T_r as can be seen in (20).

Let us see the Laplace transform $I_s(p)$ of the stator current in (5). An interesting determination from (5) can be expressed as follows:

- The Laplace transform of the stator current $I_s(p)$ in (5) is not a single-valued function. The Laplace transform in (5) remains unchanged even if the rotor circuit has an arbitrary self-inductance L_{rx} , but it meets the condition of having the same time constant $T_r = L_r/R_r$ and the same leakage factor σ as in the original case.
- When we arbitrarily change self-inductance L_r into L_{rx} , we must also change the resistance R_r into R_{rx} to ensure that the new set of rotor winding parameters has the same time constant T_r as the original one.

The rotor time constant T_r remains the same after a change of L_r and R_r when the substitute rotor resistance is calculated according to the following relation:

$$R_{rx} = \frac{L_{rx}}{T_r} = \frac{L_{rx}}{L_r} R_r. \quad (22)$$

It means that the ratio R_{rx}/R_r must be the same as the ratio L_{rx}/L_r .

A change of L_r into L_{rx} causes a change of the mutual inductance M into M_x . But the leakage factor σ must remain unchanged. Therefore, let us change L_r into L_{rx} and set it equal to L_s . Then, we get, according to (21), the same σ as in the original case for the new mutual inductance.

$$M_x = \sqrt{L_s L_{rx} (1 - \sigma)} = L_s \sqrt{1 - \sigma}. \quad (23)$$

Using this method, we can choose the self-inductance L_{rx} quite arbitrarily and find a substitute rotor winding. Let us call the substitute parameters all the members of the new set with the changed

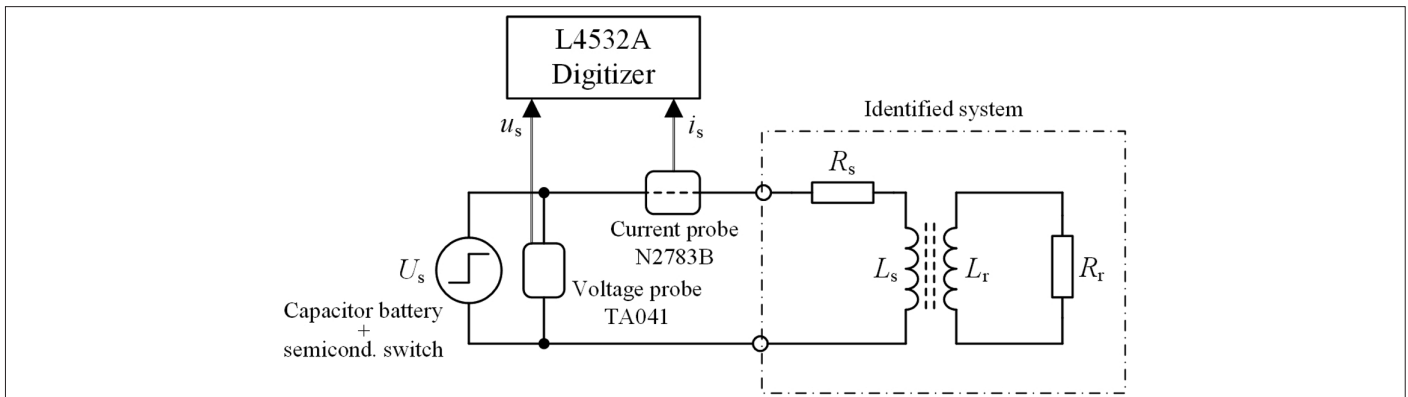


Fig. 1. The scheme of the measurement of two coupled windings.

rotor winding parameters that have the same influence on the stator winding as the original one. The substitute parameters have the same influence on the current $i_s(t)$ because its Laplace transform $I_s(p)$ remains unchanged.

We accurately identified the rotor parameters in the exploitable form of the set of substitute parameters, although the particular parameters L_r , R_r , and M are unknown, without access to the rotor circuit. It is sufficient to determine the stator parameters L_s and R_s that are not complicated to measure and calculate, as mentioned above, and two time constants T_2 and T_3 . The determination of the time constants is described in Chapter III.

III. EXPERIMENTAL VERIFICATION OF IDENTITY BETWEEN THE ORIGINAL AND SUBSTITUTE SET OF PARAMETERS

To calculate the rotor time constant T_r (19), the determination of time constants T_2 and T_3 is necessary. How to determine them is described in this chapter. The measurement of an induction motor is described in Section IV.B.

A. Parameters Identification Experiment on Two Coupled Windings

We have used an experimental model to verify the method of creating the substitute rotor-winding parameters, which have the same influence on the stator winding as the original rotor winding in a standstill. The experimental model consists of two windings, each for 25 A, that behave like a transformer with an air gap. The primary winding is used as a model for one phase of the stator winding, and the secondary winding as a model for the short-circuited squirrel cage winding of an induction machine. The parameters of both windings are fixed and firmly given by the construction and the winding temperature. Both windings of the experimental device have only mutual magnetic coupling and can be described by (1) and (2).

The electrical scheme of the measurement is depicted in Fig. 1. R_s represents the stator (primary) resistance and R_r stands for rotor (secondary) resistance, which can be adjusted as needed. The primary side is supplied from the voltage source (capacitor battery) by voltage step u_s . Let us apply the voltage step $u_s = 1 \cdot U_s = 1 \cdot 13.6$ V. It is done by a transistor switch. The response, i.e., the stator current, was recorded with a digital electronic instrument L4532A Digitizer (16-bit ADC resolution) as $i_s(t)$, and it is shown in Fig. 2. The voltage pulse was recorded as well.

According to (10), the waveform of the stator current $i_s(t)$ consists of three components. The first component in (10) is valid for $p_1 = 0$, and it is the steady-state component I_{∞} . The second component of the current is the transient component (see Fig. 3).

$$i_s^* = I_{\infty} - i_s = A_2 e^{p_2 t} + A_3 e^{p_3 t}. \quad (24)$$

The transient component is a sum of two exponential curves that are shown in Fig. 4. (More precisely, it is a series of digital values that represents two exponential curves in Fig. 4 — red and black.) As already mentioned, constants p_2 and p_3 are negative, and they can be replaced by time constants T_2 and T_3 , respectively. The decomposition of the transient component i_s^* into two exponential curves was performed with the help of the function *fit* of the *Curve Fitting Toolbox* in MATLAB [42]. The decomposition algorithm requires both the input voltage signal and the current response. The decomposition is shown in Fig. 4 as well.

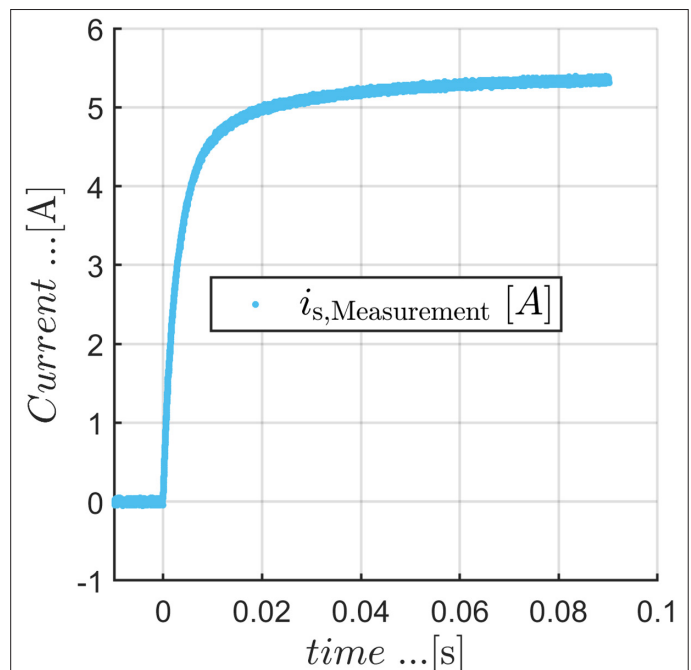


Fig. 2. Step response of the stator current $i_s(t)$.

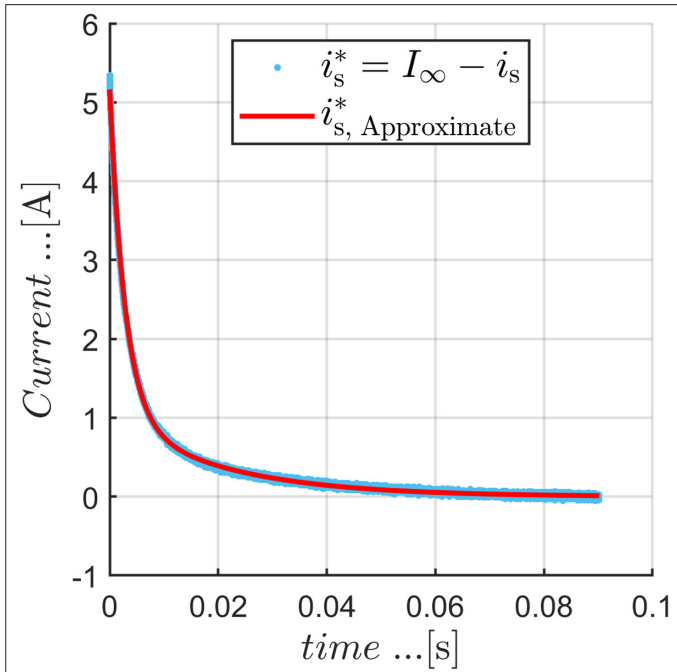


Fig. 3. The transient component of the stator current $i_s^*(t)$, i.e., $i_s^* = I_\infty - i_s$.

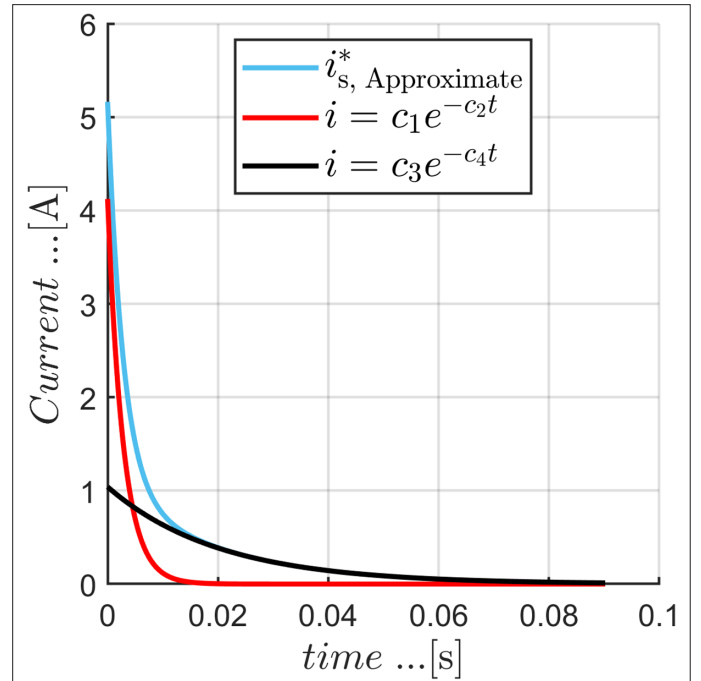


Fig. 4. Two exponential curves (black and red) make up the transient component i_s^* (blue).

The known, measured, and calculated parameters of the experimental windings are taken down in Table 1.

The entire process is depicted in the flowchart in Fig. 5.

B. Results Verification

The results of the identification method need to be verified to ensure they are correct. Let us verify it using the following calculation. We expect that our system described by (1) and (2), parameterized according to Table 1 and excited with the voltage step $u_s = \underline{1} \cdot U_s = \underline{1} \cdot 13.6 \text{ V}$, will result in the same waveform $i_s(t)$ as the measured waveform in Fig. 2.

The calculation will be done numerically by the Runge-Kutta method on a computer. Equations (1) and (2) can be rewritten into the form that is suitable for this numerical calculation as

$$L_s \frac{di_s}{dt} + M \frac{di_r}{dt} = -R_s \cdot i_s + u_s, \quad (25)$$

$$M \frac{di_s}{dt} + L_r \frac{di_r}{dt} = -R_r \cdot i_r. \quad (26)$$

For computer calculation, the matrix form of (25) and (26) would be better. Thus, let us write

$$\mathbf{L} \begin{pmatrix} \frac{di_s}{dt} \\ \frac{di_r}{dt} \end{pmatrix} = -\mathbf{R} \begin{pmatrix} i_s \\ i_r \end{pmatrix} + \begin{pmatrix} u_s \\ 0 \end{pmatrix}, \quad (27)$$

$$\mathbf{L} = \begin{pmatrix} L_s & M \\ M & L_r \end{pmatrix}, \quad (28)$$

$$\mathbf{R} = \begin{pmatrix} R_s & 0 \\ 0 & R_r \end{pmatrix}, \quad (29)$$

TABLE 1. KNOWN, MEASURED, AND CALCULATED PARAMETERS OF THE EXPERIMENTAL WINDINGS. THE VOLTAGE STEP ON THE EXPERIMENTAL WINDING WAS APPLIED AT 20°C.

	Name	Symbol	Value
Known	Voltage step	U_s [V]	13.6
	Known stator resistance	R_s [Ω]	2.543
	Known stator self-inductance	L_s [H]	0.0172
Obtained by current response decomposition (i.e. measured)	Measured time constant (decomposition)	T_2 [ms]	20.20
	Measured time constant (decomposition)	T_3 [ms]	2.81
Arbitrarily chosen	Chosen substitute rotor self-inductance	L_{rx}	L_s
Calculated	Stator time constant (8)	T_s [ms]	6.76
	Rotor time constant (19)	T_r [ms]	16.25
	Inductive leakage factor (20)	σ [-]	0.517
	Substitute rotor resistance (22)	R_{rx} [Ω]	1.058
	Substitute mutual inductance (23)	M_x [H]	0.0119

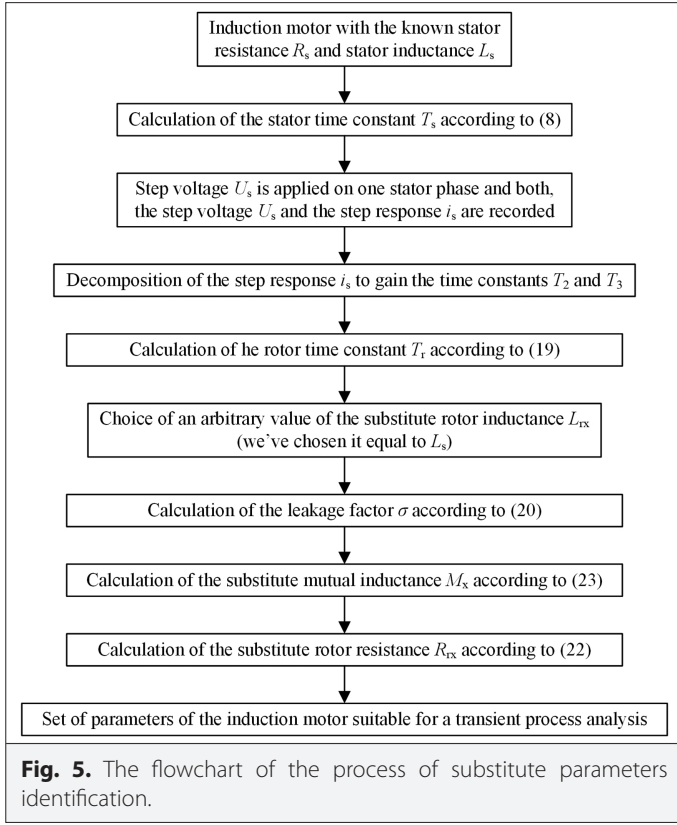


Fig. 5. The flowchart of the process of substitute parameters identification.

$$\begin{pmatrix} \frac{di_s}{dt} \\ \frac{di_r}{dt} \end{pmatrix} = -\mathbf{L}^{-1}\mathbf{R} \begin{pmatrix} i_s \\ i_r \end{pmatrix} + \mathbf{L}^{-1} \begin{pmatrix} U_s \\ 0 \end{pmatrix} = \mathbf{A} \begin{pmatrix} i_s \\ i_r \end{pmatrix} + \mathbf{B} \begin{pmatrix} U_s \\ 0 \end{pmatrix}, \quad (30)$$

We do not use the rotor circuit parameters of the experimental winding because we assume that a real rotor of an induction machine is inaccessible. That is why the substitute parameters R_{rx} and M_x defined in (22) and (23) and enumerated in Table 1 must be used. When we use the substitute inductance L_{rx} instead of self-inductance L_r , the substitute resistance R_{rx} instead of R_r and the substitute mutual inductance M_x instead of M in (28)–(30), we get the current waveform depicted in Fig. 6.

When we compare the measured current waveform in Fig. 2 with the calculated one in Fig. 6, we can see that they are identical. Thus, the dynamic analysis can be performed with the set of substitute parameters obtained according to our method.

Let us repeat the winding substitute parameters once more:

- Arbitrary substitute rotor self-inductance $L_{rx} = L_s$.
- Substitute mutual inductance $M_x = L_s \sqrt{1 - \sigma}$.
- Substitute rotor resistance $R_{rx} = L_{rx} / T_r$.

C. Another Results Verification

Another expressive comparison can be made. Let us use a similar way of calculating the step response as in Section III.B; however, for two different arbitrarily chosen rotor self-inductances $L_{rx} = L_s$ (case 1) and $L_{rx} = 2 \cdot L_s$ (case 2). The chosen parameters, as well as calculated parameters M_x and R_{rx} for both cases, are stated in Table 2.

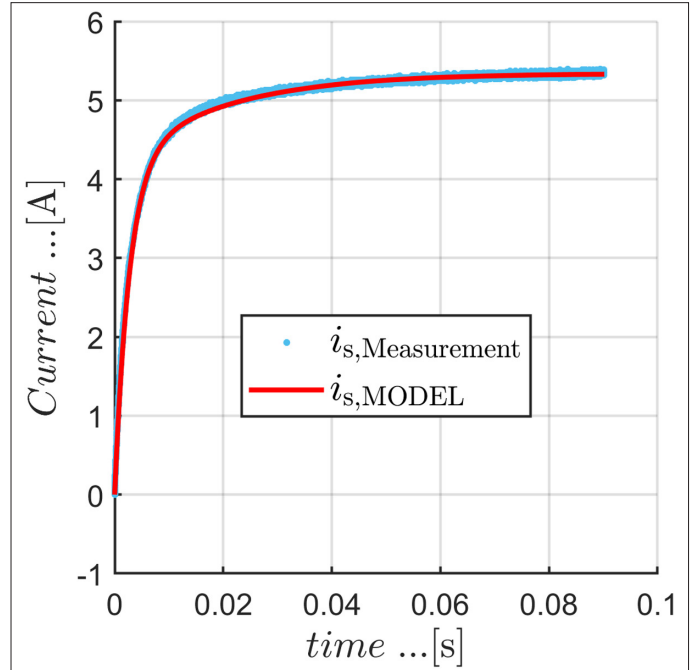


Fig. 6. The calculated step response of the stator current when the identified substitute parameters are used (red curve). The blue curve is the measured step response, the same one as in Fig. 2.

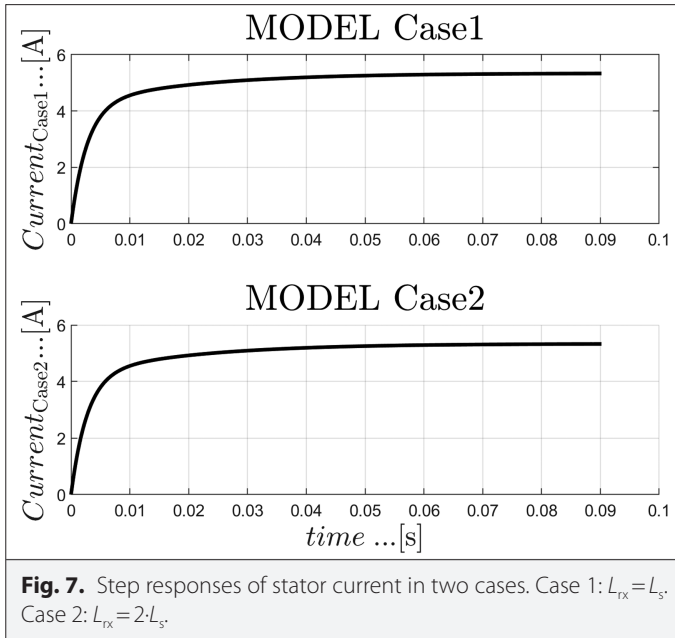
Step responses of both systems are depicted in Fig. 7. The waveforms are identical. Thus, it is apparent that the rotor self-inductances may be arbitrarily chosen, as was described in Section III.A.

IV. EXACT DETERMINATION OF INDUCTION MACHINE ROTOR TEMPERATURE RISE

The laboratory measurement of the machine-winding temperature is very important. This is because the lifetime of a machine depends

TABLE 2. TWO DIFFERENT SETS OF SUBSTITUTE WINDING PARAMETERS

Name	Symbol	Case 1	Case 2
Voltage step	U [V]	13.6	13.6
Known stator resistance	R_s [Ω]	2.543	2.543
Known self-inductance	L_s [H]	0.0172	0.0172
Stator time constant (8)	T_s [ms]	6.76	6.76
Measured time constant (decomposition)	T_2 [ms]	20.20	20.20
Measured time constant (decomposition)	T_3 [ms]	2.81	2.81
Chosen substitute rotor self-inductance	L_{rx} [H]	0.0172	0.0344
Rotor time constant (19)	T_r [ms]	16.25	16.25
Inductive leakage factor (20)	σ [–]	0.517	0.517
Substitute rotor resistance (22)	R_{rx} [Ω]	1.058	2.117
Substitute mutual inductance (23)	M_x [H]	0.0119	0.0169



very closely on the temperature to which the insulation material is exposed during its lifetime. Therefore, the heat-run test is one of the most important producer's and client's interests during the acceptance tests.

For the measurement of the rotor resistance, access to the winding is necessary. In the case of an induction motor with a rotor squirrel cage winding, access for the measurement of the rotor cage winding is complicated and, we can say, impossible.

A. Theoretical Determination of Rotor Temperature Rise with Use of the Proposed Method

It is mentioned in Section II.C that the real stator transient current $i_s(t)$ response to the DC voltage step U_s depends on three time constants T_1, T_2, T_3 , or three exponents p_1, p_2, p_3 . Because T_3 is known or can be measured, we can obtain T_r from (19) in the cold state and in the warm state. All time constants depend on the temperature and on the magnetic flux. The influence of the time constants by magnetic flux decreases with the decreasing of the magnetic flux. Based on practice, the inductance of one phase can be considered to be constant if the magnetic flux corresponds with a magnetizing current around 10% of the nominal current of the machine. If the inductance of one phase is constant, then the time constant depends only on the temperature of one phase. Thus, it is necessary to measure T_r with such low current, i.e., under a sufficiently low voltage. Further, we must measure T_r two times in the machine: in the cold state of the machine first and in the warm state afterward. The measurement in the warm state must be performed when the warming reaches its final value, i.e., after the transient process is over. Because the inductance does not change with the temperature, it is sufficient to write the following equation where $T_r = L_r/R_r$ is used in both the cold state and the warm state as well.

$$\frac{T_{rcold}}{T_{rwarm}} = \frac{R_{rwarm}}{R_{rcold}}. \quad (31)$$

This means measuring only the ratio T_{rcold}/T_{rwarm} according to (19) and then calculating the ratio R_{rwarm}/R_{rcold} according to (31). Notice again

that access to the stator winding is sufficient; we do not need to perform any measurements on the rotor winding.

To measure the temperature rise during the load test, two measurements must be performed: T_r in the cold state, i.e., at 20°C, to get the time constant T_{rcold} , and T_r in the warm state to get the time constant T_{rwarm} . Because the resistance depends on the temperature linearly as

$$\frac{R_{rwarm}}{R_{rcold}} = 1 + \alpha(\vartheta_{warm} - \vartheta_{cold}), \quad (32)$$

where α is the temperature coefficient of resistance (TCR) and ϑ_{warm} and ϑ_{cold} are the temperatures in the warm state and cold state, respectively, it can be written using (31) for the temperature rise $\Delta\vartheta$.

$$\Delta\vartheta = \vartheta_{warm} - \vartheta_{cold} = \frac{\frac{T_{rcold}}{T_{rwarm}} - 1}{\alpha}. \quad (33)$$

Thus, the method of substitute parameter identification described in Chapter II. enables us to determine the temperature rise of the inaccessible rotor winding of the induction machine.

B. Experimental Verification

The experimental determination of rotor time constants T_{rcold} and T_{rwarm} from (33) according to the proposed method was performed on the induction motor with the nominal parameters and basic measured parameters that are listed in Table 3.

The experimental setup is similar to the arrangement depicted in Fig. 1, but the identified system is the star-connected induction motor instead of the experimental model, and it is supplied between one phase terminal and the neutral point of the motor. The picture of the setup is in Fig. 8. The measurement of the stator current response described in Section III.A was done several times on the induction motor. The voltage step u_s had the value $u_s = 1 \cdot U_s = 1 \cdot 3.077 \text{ V}$ to ensure the measurement in the linear part of the magnetizing characteristic. The initial measurement was done in the cold state at room temperature $\vartheta_{meas} = 24^\circ\text{C}$ by a thermocouple, and the rotor time constant T_{rcold} was calculated. After this measurement, the induction motor was loaded by a certain load until it reached the stable temperature $\vartheta_{meas} = 74^\circ\text{C}$, which was measured by a thermocouple on its rotor aluminum ring. In order to calculate the temperature rise at different temperatures, the step responses were recorded during the spontaneous cooling of the standing motor and decomposed to obtain time constants T_2 and T_3 . The measurement of the temperature of the

TABLE 3. PARAMETERS OF THE EXPERIMENTAL INDUCTION MACHINE

Nominal power	0.75 kW
Nominal voltage (Y)	380 V
Nominal current	2 A
Nominal speed	1380 rpm
Nominal power factor	0.79
Stator resistance R_s (at 24 °C)	10.66 Ω
Stator self-inductance L_s	0.44 H

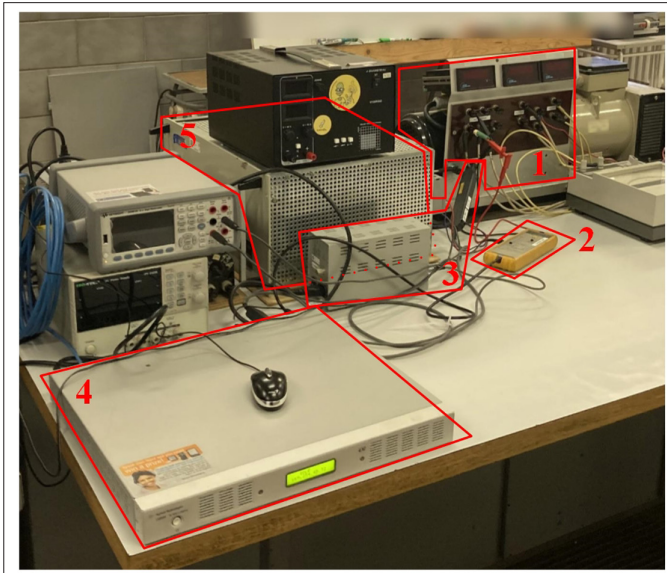


Fig. 8. Experimental setup (1—Induction motor, 2—Voltage probe Pico Technology TA041, 3—Current probe Keysight N2783B with its source, 4—Digitizer Agilent L4532A, 5—Capacitor battery with semiconductor switch).

rotor aluminum ring was done as well. At last, the rotor time constant T_{warm} for each case was calculated according to (19) as well as the temperature rise $\Delta\vartheta_{\text{calc}}$ according to (33). The summary of some measured and calculated values is given in Table 4. TCR of aluminum is 0.004 K^{-1} [43].

Table 4 also contains the difference between the temperature rise measured by a thermocouple, $\Delta\vartheta_{\text{meas}}$, and temperature rise $\Delta\vartheta_{\text{calc}}$ calculated according to (33). However, the results cannot be compared with published results due to their lack in the literature

because rather the comparison of temperature (not temperature rise) is presented in relation to this problem. That is why there are the last two rows in Table 4 — the calculated temperature, ϑ_{calc} (i.e., room temperature plus calculated temperature rise), and the relative error of the temperature determination. The relative errors are acceptably low, and they are within the confines of accuracy as in [31] or [33].

As an example of a measured waveform, the current step response is shown in Fig. 9. The blue waveform was measured at the temperature $\vartheta_{\text{meas}} = 50.2^\circ\text{C}$. Just as in the case of the numerical verification in Section III.B, the substitute parameters were used for the numerical calculation, this time for the calculation of the rotor-locked induction machine excited by the step voltage $u_s = 1.3.077 \text{ V}$ in one phase. The result of the calculation is the current step response, and it is shown as the red dashed waveform in Fig. 9 together with the measured one. Both waveforms differ minimally; they are identical, practically. It is another verification that the presented method of substitute parameters identification is correct.

The accuracy of the identification method depends on several factors. The first one is the precision of the current and voltage measurement and the resolution of the recording device used, e.g., digitizer. 16-bit resolution digitizer is recommended. Measurements with devices of lower resolution did not achieve satisfactory results, so resolution is a crucial issue. The second factor is how precisely the value of the stator inductance is determined. It is hard to present the sensitivity analysis as the quantities are mutually correlated. In addition, the method assumes that the inductance does not depend on temperature, and it is often considered thermally independent in technical practice. However, the inductance varies very slightly in the common range of temperatures at which induction machines usually work. Our calculations showed that a thermal dependence of the inductance affects the relative error of the temperature determination in the order of percentage units. The last factor is the TCR. The cages of induction machines are mostly manufactured from

TABLE 4. SUMMARY OF MEASURED AND CALCULATED VALUES

T_i index	Cold Init. meas.	Warm			
		Meas. 1	Meas. 2	Meas. 3	Meas. 4
ϑ_{meas} ($^\circ\text{C}$)	24.0	74.0	54.2	50.2	45.0
R_s (Ω)	10.659	12.894	12.286	12.033	11.747
T_2 (s)	0.119942	0.101024	0.106250	0.108499	0.111168
T_3 (s)	0.006210	0.005248	0.005500	0.005615	0.005757
T_5 (s)	0.040762	0.034396	0.036182	0.036903	0.037865
T_r (s)	0.08539	0.071876	0.075568	0.077211	0.079060
$\Delta\vartheta_{\text{meas}}$ ($^\circ\text{C}$)	---	50.0	30.2	26.2	21.0
$\Delta\vartheta_{\text{calc}}$ ($^\circ\text{C}$)	---	47.0	32.5	26.5	20.8
$\Delta\vartheta_{\text{meas}} - \Delta\vartheta_{\text{calc}}$ ($^\circ\text{C}$)	---	-3.0	2.3	0.3	-1.7
Relative error of the temperature rise $\Delta\vartheta$	---	-6.0 %	7.6 %	1.1 %	-4.7 %
ϑ_{calc} ($^\circ\text{C}$)	---	71.0	56.5	50.5	44.0
Relative error of the temperature ϑ	---	4.0 %	-4.2 %	-0.6 %	2.2 %

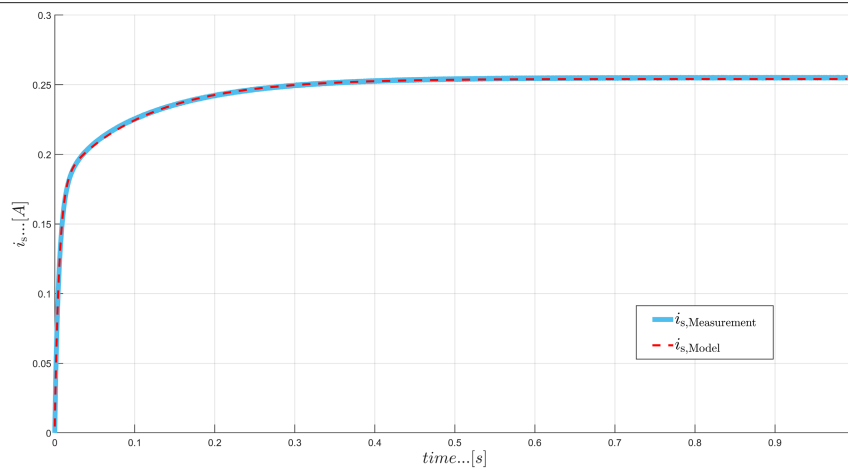


Fig. 9. The calculated step response of the induction motor stator current when the identified substitute parameters are used (red dashed curve). The blue curve is the measured step response.

aluminum; however, some producers use aluminum alloys that have slightly different values of TCR [44].

V. CONCLUSION

In this paper, the method for the identification of a set of substitute parameters of a still-standing induction machine is presented. An induction machine described with such a set of substitute parameters evinces the same responses of transient processes as with the set of real parameters. Thus, the transient processes can be analyzed. To perform this method, it is required to excite one phase of an induction machine with a voltage step that will cause a sufficiently low current response in order to measure in an unsaturated state. The current response, as well as the step voltage signals, have to be recorded with a digitizer. Afterward, the current response is decomposed to obtain several time constants. Using the obtained time constants with known stator resistance and stator inductance, the substitute parameters can be determined. Moreover, the temperature rise of the rotor cage can be calculated.

The identification method was also verified. Firstly, the measurement on two coupled windings representing a still-standing induction machine was done, and the results were verified in two different ways by calculation. Secondly, the measurement was performed on an induction machine to prove that our method is suitable for determining the temperature rise. The relative error of the temperature rise does not exceed 8%. After the recalculation for the temperature determination, the relative error does not exceed 5%. This verification also shows a practical usage of the presented method. The method allows us to determine the temperature rise of a rotor winding of an induction machine with acceptable accuracy in practice and in a quite a simple way, which is the advantage of the method. The described method is so simple that the temperature rise of the rotor can be measured immediately after a ride with an electric vehicle without regard to the way of driving, i.e., not in a testing laboratory. The acquired information is usable, e.g., by design engineers of traction drives.

Availability of Data and Materials: The data that support the findings of this study are available on request from the corresponding author.

Peer-review: Externally peer-reviewed.

Author Contributions: Concept – P.K., Z.Č.; Design – Z.Č., M.L.; Supervision – Z.Č.; Materials – M.L.; Data Collection and/or Processing – M.L.; Analysis and/or Interpretation – P.K.; Literature Search – Z.Č.; Writing – P.K., Z.Č.; Critical Review – P.K.

Declaration of Interests: The authors have no conflict of interest to declare.

Funding: The authors declared that this study has received no financial support.

REFERENCES

1. J. Tang, Y. Yang, F. Blaabjerg, J. Chen, L. Diao, and Z. Liu, "Parameter identification of inverter-fed induction motors: A review," *Energies*, vol. 11, no. 9, pp. 1–21, 2018. [\[CrossRef\]](#)
2. F. J. Lin, and M. S. Su, "A high-performance induction motor drive with on-line rotor time-constant estimation," *IEEE Trans. Energy Convers.*, vol. 12, no. 4, pp. 297–303, 1997. [\[CrossRef\]](#)
3. P. Vas, *Parameter Estimation Condition Monitoring and Diagnosis of Electrical Machines*. Oxford, UK: Clarendon Press, 1993.
4. T. Kořtál, and P. Koblre, "Induction machine on-line parameter identification for resource-constrained microcontrollers based on steady-state voltage model," *Electronics*, vol. 10, no. 16, pp. 1–19, 2021.
5. B. Heller, and A. Veverka, "Surge phenomena in electric machines," *Verlag Tech., Berlin, Federal Republic of Germany*, 1957.
6. H. O. Seinsch, "Principles of electric Machinery and drives," *B. G. Teubner, Stuttgart, Federal Republic of Germany*, 1993.
7. Z. Čeřovský, "Käfigströme und Käfigverluste der Stromrichter motoren," *Arch. Elektrotech.*, vol. 64, no. 6, pp. 341–348, 1982. [\[CrossRef\]](#)
8. H. O. Seinsch, "Transient phenomena in AC machines," *B. G. Teubner, Stuttgart, Federal Republic of Germany*, 1991.
9. N. Erdogan, H. Henao, and R. Grisel, "The analysis of saturation effects on transient behavior of induction machine direct starting," *IEEE International Symposium on Industrial Electronics, Ajaccio, France, May 4–7, 2004*, pp. 975–979 vol. 2. [\[CrossRef\]](#)
10. V. R. Cociu, and L. Cociu, "Transient short circuit currents and fluxes expressions of induction machines," in *International Conference and Exposition on Electrical and Power Engineering, EPE 2014, Iasi, Romania, October 16–18, 2014*, 2014, pp. 381–385. [\[CrossRef\]](#)
11. Y. Chen, W. Xu, Y. Liu, Z. Bao, Z. Mao, and E. M. Rashad, "Modeling and transient response analysis of doubly-fed variable speed pumped storage unit in pumping mode," *IEEE Trans. Ind. Electron.*, vol. 70, no. 10, pp. 9935–9947, 2023. [\[CrossRef\]](#)
12. E. Armando, A. Boglietti, F. Mandrile, E. Carpaneto, and S. Rubino, "A detailed analysis of the electromagnetic phenomena observed during the flux-decay test," in *International Conference on Electrical Machines, ICEM 2022, Valencia, Spain, September 5–8, 2022*, 2022, pp. 767–773. [\[CrossRef\]](#)

13. D. Bíró, F. Diwoky, and E. Schmodt, "Advanced circuit approach for induction machines parametrized by field calculations," in 23rd International Conference on the Computation of Electromagnetic Fields, COMPUMAG 2023, Cancun, Mexico, January 16–20, 2022, 2022, pp. 767–773.
14. K. Takeuchi, and M. Matsushita, "Impulse response-based induction machine model for starting simulation considering deep-bar effect," *IEEE Trans. Energy Convers.*, vol. 38, no. 1, pp. 573–584, 2023. [\[CrossRef\]](#)
15. J. Bonet-Jara, J. Pons-Llinares, D. Morinigo-Sotelo, and K. N. Gyftakis, "A novel approach for early detection of inter-turn faults in induction motors during start-up," in *Power Electron. Drives 14th International Symposium on Diagnostics for Electrical Machines, SDEMPED 2023*, Chania, Greece, August 28–31, 2023. IEEE Publications, 2023, pp. 56–62. [\[CrossRef\]](#)
16. R. Rüdtenberg, *Transient Performance of Electric Power System: Phenomena in Lumped Networks*. MI, USA: M.I.T. Press, 1969.
17. K. Reichert, "A simplified approach to permanent magnet and reluctance motor characteristics determination by finite-element methods," *COMPEL Int. J. Comput. Math. Electr. Electron. Eng.*, vol. 25, no. 2, pp. 368–378, 2006. [\[CrossRef\]](#)
18. P. Han, J. Liang, P. Gottipati, and M. Solveson, "Fast 3D transient electromagnetic FEA for e-NVH analysis of induction machines," in IEEE Energy Conversion Congress and Exposition. Detroit, MI, USA: ECCE, 2022. [\[CrossRef\]](#)
19. R. Helmer, E. Garbe, J. Steinbrink, and B. Ponick, "Combined analytical-numerical calculation of electrical machines," *Acta Tech.*, vol. 25, no. 1, pp. 1–18, 2009.
20. D. Zarko, D. Ban, and T. A. Lipo, "Analytical calculation of magnetic field distribution in the slotted air gap of a surface permanent-magnet motor using complex relative air-gap permeance," *IEEE Trans. Magn.*, vol. 42, no. 7, pp. 1828–1837, 2006. [\[CrossRef\]](#)
21. "User's Manual FEMAG, Interactive program for workstations to calculate and analyse 2-dimensional and axisymmetric magnetic and eddy-currents fields," *Institut für Elektrische Maschinen*. Zürich: ETH Zürich, Swiss, 1982.
22. A. Dell'Aquila, L. Salvatore, and N. Savino, "A new test method for determination of induction motor efficiency," *Power Appar. Syst.*, vol. 10. PAS-103, pp. 2961–2973, 1984.
23. P. Coirault, J. C. Trigeassou, J. P. Gaubert, and G. Champenois, "Parameter identification of an induction machine for diagnosis," *IAFC Proc. Volumes*, vol. 30, no. 18, pp. 265–270, 1997. [\[CrossRef\]](#)
24. D. Telford, M. W. Dunnigan, and B. W. Williams, "Online identification of induction machine electrical parameters for vector control loop tuning," *IEEE Trans. Ind. Electron.*, vol. 50, no. 2, pp. 253–261, 2003. [\[CrossRef\]](#)
25. S. Khazi et al., "Analyzation of temperature rise in induction motor for electric vehicles," in *Advances in Energy Technology*. Singapore: Springer, 2022, pp. 173–183. [\[CrossRef\]](#)
26. S. Cheng, C. Li, F. Chai, and H. Gong, "Research on induction motor for mini electric vehicles," *Energy Procedia*, vol. 17, No. A, pp. 249–257, 2012. [\[CrossRef\]](#)
27. J. D. Walker, and S. Williamson, "Temperature rise in induction motors under stall conditions," in *IEE Colloquium on Thermal Aspects of Machines*, vol. 27. London, UK: October, 1992.
28. A. Boglietti, A. Cavagnino, M. Lazzari, and M. Pastorelli, "A simplified thermal model for variable-speed self-cooled industrial induction motor," *IEEE Trans. Ind. Appl.*, vol. 39, no. 4, pp. 945–952, 2003. [\[CrossRef\]](#)
29. C. Kral et al., "Rotor temperature estimation of squirrel-cage induction motors by means of a combined scheme of parameter estimation and a thermal equivalent model," *IEEE Trans. Ind. Appl.*, vol. 40, no. 4, pp. 1049–1057, 2004. [\[CrossRef\]](#)
30. Z. Gao, R. S. Colby, and L. Turner, "Induction motor rotor temperature estimation using superheterodyne receivers," IEEE Energy Conversion Congress and Exposition. Phoenix, AZ, USA: ECCE, Sept. 17-22 2011, 2011, pp. 730–738. [\[CrossRef\]](#)
31. Y. Wu, and H. Gao, "Induction-motor stator and rotor winding temperature estimation using signal injection method," in *IEEE Trans. Ind. Appl.*, vol. 42, no. 4, pp. 1038–1044, 2006.
32. K. R. Cho, and J. K. Seok, "Induction motor rotor temperature estimation based on a high-frequency model of a rotor bar," *IEEE Trans. Ind. Appl.*, vol. 45, no. 4, pp. 1267–1275, 2009.
33. Y. Du, P. Zhang, Z. Gao, and T. G. Habetler, "Assessment of available methods for estimating rotor temperatures of induction motor," in IEEE International Electric Machines and Drives Conference May 3–6 2009, Miami, FL, USA, 2009, pp. 1340–1345.
34. A. Angot, "Compléments de Mathématiques destinés aux ingénieurs de l'électrotechnique et des Télécommunications," *Rev. Optique, France*, 1952.
35. G. A. Korn, and T. M. Korn, *Mathematical Handbook for Scientists and Engineers*. New York, USA: McGraw-Hill, 1961.
36. K. W. Wagner, *Operatorenrechnung Nebst Anwendungen in Physik und Technik*. Leipzig, Germany: Johann Ambrosius Barth Verlag, 1940.
37. H. Jordan, V. Klíma, and K. P. Kovács, "Asynchronmaschinen," *Akad. Kaidó, Budapest, Hungary*, 1975.
38. M. Liwschitz, *Die Elektrischen Maschinen, Band III – Berechnung und Bemessung*. Berlin, Germany, 1934.
39. D. W. Nowotny, and T. A. Lipo, *Vector Control and Dynamics of AC Drives*. Oxford: Oxford University Press, 2000.
40. M. Lory, *Bestimmung der Reaktanzen von Turbogeneratoren mit der FE Methode* Ph.D. Thesis, Institut für elektrische Maschinen. Zürich: ETH Zürich, Swiss, 1998.
41. M. Liwschitz-Garik, and C. Whipple, *Electric Machinery, Vol. 2, A-C Machines*. New York, USA: D. Van Nostrand Co., 1948.
42. *Curve Fitting Toolbox for Use with MATLAB*. Natick, USA: The MathWorks, Incorp., 2020.
43. *Handbook of Formulae and Physical Constants*. Canada: Power Engineering Training Systems, 2003.
44. Y. Li et al., "Al alloys and casting processes for induction motor applications in battery-powered electric vehicles: A review," *Metals*, vol. 12, no. 2, pp. 1–25, 2022. [\[CrossRef\]](#)



Prof. Zdeněk Čeřovský graduated from Czech Technical University in Prague. He started his career with ČKD factory as a DC/AC machine designer. He projected hoisting engines, mill stand engines, ship engines, drives for streetcars, locos, and electric vehicles. After that, he worked as the head of Power Electronics Department at the Institute for Electrical Engineering in the Czechoslovak Academy of Sciences. He designed the first streetcar with induction motors in former Czechoslovakia together with ČKD. Before he became a professor at Czech Technical University in Prague, he was the director of the Institute for Electrical Engineering at the Czechoslovak Academy of Sciences. Nowadays, he is an emeritus professor at Czech Technical University in Prague.



Pavel Koblře received the M.Sc. and Ph.D. degrees in electrical engineering from the Czech Technical University in Prague, in 2008 and 2014, respectively. Since 2009, he has been working as an assistant professor at the Department of Electrical Drives and Traction at his alma mater. In 2013, he became a full-time lecturer there. His research interests include mathematical modeling of electrical machines, parameter identification issues, and control of power electronics converters, especially multilevel converters, for energetic systems and variable-frequency drives.



Miroslav Lev graduated from Czech Technical University in Prague twice. The first time at the Faculty of Electrical Engineering with a specialization technical cybernetics, and the second time was at the Faculty of Mechanical Engineering with a specialization production machines and equipment. For the most part of his technical career, he was employed by the Research Institute of Machine Tools and Machining (VUOSO), the factory KONE Lifts, and ITI TÜV Group Süddeutschland. At the present time, he is the assistant professor at Czech Technical University in Prague, Faculty of Electrical Engineering, Department of Electric Drives and Traction. His current interests include mathematical simulation and programming of systems working in real time.